signal in the frequency domain, to centre the interference in a subband. The filtering process is performed for every frequency shift, $d(j)$. The number of shifts is given by the bandwidth of the filters (B_J), $d(j) \in [0, \ldots, B_J]$. Thus, the output vectors using a periodic extension of the input signal are

$$W_{J,0,d(J)}(n) = \sum_{l=0}^{L-1} h_0(l)(X_{J,d(J)}(n - 2^{J-1}l)) \quad (1)$$

$$W_{J,1,d(J)}(n) = \sum_{l=0}^{L-1} g_0(l)(X_{J,d(J)}(n - 2^{J-1}l)) \quad (2)$$

where $h_0(l)$ and $g_0(l)$ are the analysis filters, L is the length of the filters and $X_{J,d(j)}$ is the frequency shifted input vector. Once the decomposition at level 'J' is done for every frequency shift, the energy difference between every pair, $W_{J,0,d(j)}$, $W_{J,1,d(j)}$, is calculated. The algorithm selects the pair with a greater energy difference, defined as:

$$\Delta E_{J,d(J)} = \left\| \sum_{n=0}^{N-1} \|W_{J,1,d(J)}(n)\|^2 - \sum_{n=0}^{N-1} \|W_{J,0,d(J)}(n)\|^2 \right\| \quad (3)$$

where N is the number of elements in $W_{J,1,d(j)}$ and $W_{J,0,d(j)}$.

The frequency shift for this selected pair is the optimum, $D(J) = \{d(J) | \max(\Delta E_{J,d(J)})\}$, and the vector with greater energy from this pair ($W_{J,0,D(j)}$ or $W_{J,1,D(j)}$) contains the interference, thus it is chosen as the new input vector X_{J-1}, at the next resolution level '$J-1$'. The other vector from the selected pair is saved together with D_J. If the energy difference is similar for all the pairs, the interference bandwidth is greater than the bandwidth of the filters at level 'J', and they cannot concentrate the whole interference. The algorithm must then start at a lower resolution level, '$J-1$'.

Once the filtering at level 'J' is done due to the scaling property between filter responses as shown in Fig. 2, the frequency shift range for the following levels is bounded to two values, $d(J-1) = \{0, B_{J-1}/2\}$. Finally, when level '1' is met, the X_0 vector, which concentrates the interference, is removed. At this step, the synthesis begins using the saved vectors, from resolution level '1' until 'J'. At each level, the frequency shift is undone to restore the interference-free original signal.

Results: Simulations have been carried out using the FH-SS receiver scheme shown in Fig. 1 and binary frequency shift keying (BFSK) modulation with five orthogonal channels. The offset between frequencies in each BFSK channel is 1 KHz and separation between channels is 2 KHz. Interference is a single continuous tone that changes its frequency and with a power 14 dB higher than that of the signal. In addition to this, the interference includes additive white Gaussian noise of 12 dB SNR. Results have been obtained from 595×10^3 transmitted bits with a confidence interval of 5×10^{-5} and a confidence level of a 99%.

Fig. 3 shows the probability of error (Pe) for three design alternatives: without any excision filter (traditional scheme), with an FFT and UWPT excision filter. The Pe is measured against the frequency offset between signal and interference, from 0 to the channel central frequency (F_c).

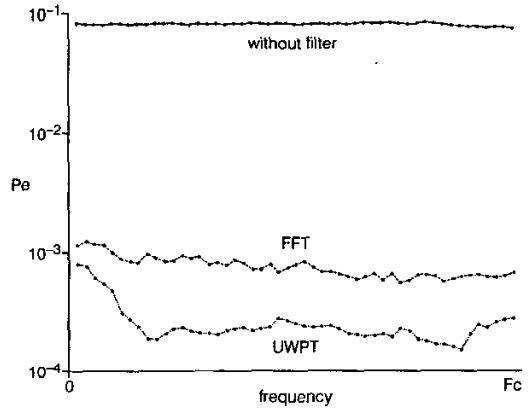

Fig. 3 *Probability of error against interference frequency offset for three excision filter schemes (without excision filter, with FFT, with UWPT filter)*

Results show the good performance of the system with the proposed parameters. The maximum probability of error (Pe) is 0.0009 against the traditional scheme, with a minimum Pe of 0.08. In addition, the Pe for the FFT excision filter is greater for all the frequencies; but the Pe difference between the two transforms is reduced for frequency offsets close to 0. This is due to the proximity of the interference to the signal, and both transforms in this case degrade the FH-SS signal.

Conclusions: An excision algorithm based on UWPT has been presented to remove narrow bandwidth interferences in FH-SS systems. Results from one experiment are provided, demonstrating the performance of the algorithm. Other experiments with different parameters have been performed to confirm the validity of the algorithm for the general case. Our conclusion is that this is a robust interference avoidance algorithm suitable for FH-SS systems.

30 November 2001
Electronics Letters Online No: 20020583
DOI: 10.1049/el:20020583

J.J. Pérez and S. Felici (*Institut de Robòtica, Universitat de València, Polígono de la Coma s/n, 46980, Paterna, Spain*)

M.A. Rodríguez (*Instituto ITACA, Universidad Politécnica de Valencia, Camino de Vera s/n, 46022, Valencia, Spain*)

References

1 CHEUN, K., and STARK, W.E.: 'Performance of FHSS systems employing carrier jitter against one-dimensional tone jamming', *IEEE Trans. Commun.*, 1995, **43**, (10), pp. 2622–2629
2 MILSTEIN, L.B.: 'Interference rejection techniques in spread-spectrum communications', *Proc. IEEE*, 1988, **76**, (6), pp. 657–671
3 TAZEBAY, M.V., and AKUNSU, A.N.: 'Adaptative subband transforms in time-frequency excisers for DS-SS communications systems', *IEEE Trans. Signal Process.*, 1995, **43**, (11), pp. 2776–2782
4 DAVIDOVIVI, S., and KANTERARAKIS, E.: 'Radiometric detection of direct-sequence spread-spectrum signals using interference excision', *IEEE J. Sel. Areas Commun.*, 1989, **7**, (4), pp. 576–588
5 SHENSA, M.: 'The discrete wavelet transform: wedding the Trous and Mallat algorithms', *IEEE Trans. Signal Process.*, 1992, **40**, (10), pp. 2464–2482
6 DAUBECHIES, I.: 'Ten lectures on wavelets' (Society for Industrial and Applied Mathematics, Philadelphia, PA, USA, 1992)

PAPR reduction of OFDM signals using multiamplitude CPM

I.A. Tasadduq and R.K. Rao

A major drawback with an orthogonal frequency division multiplexing (OFDM) system is its high peak-to-average-power ratio (PAPR). Here, the use of multiamplitude continuous phase modulation (CPM) signals for reducing PAPR is proposed and investigated. In this method, two signal points represent the same information and the one that minimises PAPR is chosen. The concept of partial transmit sequences (PTS) is used to select the best signal points. It is shown through simulations that the proposed scheme reduces the PAPR of 128-carrier OFDM-CPM signals by >4 dB.

Introduction: Orthogonal frequency division multiplexing (OFDM) has become a good candidate for wireless multimedia communication by virtue of its excellent properties in frequency-selective fading environments. In OFDM, data is transmitted over several parallel low data rate channels which provides data integrity due to fading, relative to modulation methods that employ a single channel for high data rate transmission. However, OFDM suffers from high peak-to-average-power ratio (PAPR). As the number of sub-carriers increases, the effective waveform of an OFDM signal approaches that of a sample function from a Gaussian process. This results in occasional peaks in the transmitted signal. PAPR is a good measure of these peaks. A baseband OFDM signal with N sub-channels has a $PAPR = N$. It is desired to reduce PAPR, otherwise the high peaks will be clipped, which would increase the probability of symbol error. A number of

methods have been suggested to alleviate the problem of PAPR that employ partial transmit sequences (PTS) [1, 2], block codes [3, 4] and enlarging the QAM constellation size [5].

In this Letter we introduce a new class of OFDM continuous phase modulation (OFDM-CPM) signals that use the concept of correlated phase states of a CPM signal. One of the advantages of OFDM-CPM signals is that it is possible to systematically introduce correlation amongst adjacent OFDM symbols by an appropriate choice of a parameter h. As shown in Fig. 1, serial bit stream b_i, $i=0, 1, 2,\ldots,$ with bit duration of T_b seconds is converted into blocks of N bits represented by $a_{k,p}$; $k=0, 1, 2,\ldots,$ and $p=0, 1, 2,\ldots, N-1$, where N denotes the number of carriers and $a_{k,p}=\pm 1$. For example, $a_{0,p}$ would denote the first block of N bits and $a_{1,p}$ the second block of N bits and so on. The CPM mappers transform the incoming $\{a_{k,p}\}$ into appropriate complex numbers $\{c_{k,p}\}$, i.e.

$$c_{k,p} = \cos(\theta_{k,p}) + j\sin(\theta_{k,p}) \tag{1}$$

with

$$\theta_{k,p} = a_{k,p}\pi h + \pi h \sum_{q=0}^{k-1} a_{q,p} + \phi \tag{2}$$

where parameter h defines the CPM mapper and ϕ represents the initial mapping point.

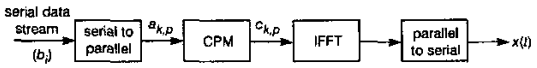

Fig. 1 *OFDM-CPM transmitter*

We present a method that uses multiamplitude CPM signals and partial transmit sequences to reduce the PAPR of OFDM-CPM signals. Unlike other PAPR reduction schemes such as partial transmit sequences, our method does not require side information to be sent to the receiver. We show that a gain of >4 dB in PAPR is possible with little complexity.

We first describe multiamplitude CPM signals. The PAPR reducing strategy is then applied, which provides good performance at lower cost and complexity.

Multiamplitude CPM signals: A typical OFDM symbol is represented by:

$$x(t) = \sum_{n=0}^{N-1} X_n e^{j2\pi f_n t},\ 0 \le t \le NT \tag{3}$$

where X_n, $\{n=0, 1,\ldots, N-1\}$, are the outputs of the mapper, f_n is the frequency of nth carrier, T_b is the original bit period and N is the number of orthogonal carriers. PAPR is defined as [2]:

$$PAPR = \frac{\max|x(t)|^2}{E[|x(t)|^2]} \tag{4}$$

In a typical OFDM system, the mapper is either PSK, DPSK, DAPSK or QAM. In this work, we consider the mapper to be CPM.

In single carrier communications, multiamplitude CPM is a generalisation of conventional CPM in which the signal amplitude is allowed to vary over a set of amplitude values while the phase of the signal is constrained to be continuous [6]. In this Letter, we use two-component CPM constellations in the mapper to reduce PAPR where the signal amplitude is allowed to take one of the two possible values. Fig. 2 shows two-component CPM constellation for two values of $h=1/2$ and $h=2/3$. The solid dots on the inner circle indicate mapping points generated by CPM mappers while the open dots on the outer circle are alternate signal points representing the same information as the solid dots lying on the same axis. Hence, each solid dot has an alternate open dot that could be chosen if it would reduce PAPR.

At the receiver the signal is decoded based on the phase of complex numbers. This eliminates the need to send additional information to the receiver about the amplitudes of complex numbers.

Proposed algorithm: Similar to the suboptimal PTS approach presented in [2], the data block which is input to IFFT is partitioned into disjoint sub-blocks or clusters. Let this input vector be represented by $X=[X_0, X_1,\ldots, X_{N-1}]^T$. Assuming that we wish to use M disjoint sub-blocks of equal size, partition the block X into M disjoint sub-blocks represented by Y_m, $m=1, 2,\ldots, M$, i.e. all sub-carrier positions in Y_m which are already represented in another sub-block are set to zero. Mathematically,

$$X = \sum_{m=1}^{M} Y_m \tag{5}$$

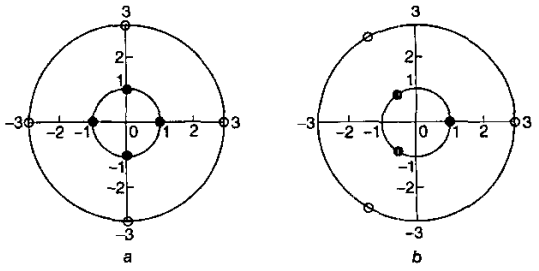

Fig. 2 *Signal space diagram for two-component CPM*
a $h=1/2$
b $h=2/3$
• mapping points generated by CPM mappers
o alternate signal points

We now need to determine which of the M sub-blocks should have their amplitudes expanded as shown in Fig. 2. Let a_m be a factor which is 3 if the amplitude of sub-block m is to be expanded and 1 if it is to remain the same. Then,

$$X' = \sum_{m=1}^{M} a_m Y_m \tag{6}$$

and in the time domain,

$$x' = \sum_{m=1}^{M} a_m.\mathrm{IFFT}\{Y_m\} = \sum_{m=1}^{M} a_m x_m \tag{7}$$

In (7), the linearity of *IFFT* is exploited.

To being, assume that $a_m=1$ for all m and compute x' using (7) and then calculate the resulting PAPR. Expand the amplitudes of elements of the first block by setting a_1 equal to 3 and recompute PAPR. If the new PAPR is less than the one in the previous step, retain the new amplitudes otherwise a_1 goes back to 1. The algorithm continues until all the possible M blocks are explored in this fashion.

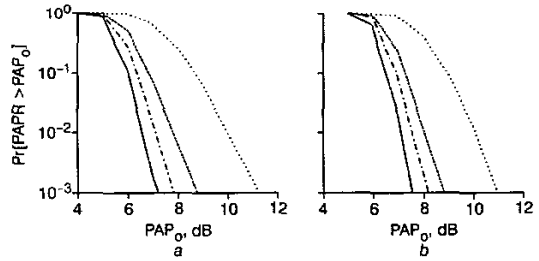

Fig. 3 *Complementary cumulative distribution function of 128-carrier OFDM-CPM system for various number clusters*
a $h=1/2$
b $h=2/3$

Fig. 3 shows the complementary cumulative distribution function (CCDF) of a 128-carrier OFDM-CPM system with $h=1/2$ and $h=2/3$ when the proposed algorithm is used. The simulation was run for 10 000 OFDM blocks and the transmitted signal was oversampled by a factor of four which is sufficient to capture the peaks. It can be seen that the PAPR for $h=1/2$ is marginally better than for $h=2/3$ when using the proposed algorithm. We investigated PAPR performance for a number of h values and found that the PAPR performance for various values of h differs only slightly. This gives additional advantage as the system designer need not worry about PAPR performance while choosing a particular value of h. For $h=1/2$, the unmodified OFDM signal has a PAPR of 11.24 dB for 0.1% of the blocks. Using the

proposed scheme with eight clusters, the 0.1% PAPR reduces to 8.78 dB, a gain of 2.46 dB. As we increase the number of clusters, PAPR reduces even further and for 32 clusters the 0.1 PAPR is 7.20 dB, a gain of 4.04 dB.

Although we have demonstrated the usefulness of the proposed algorithm for OFDM-CPM signals, the algorithm can also be used for typical OFDM signals with PSK or QAM mappers. The PSK constellation can be expanded in the same way as the CPM constellation is expanded to obtain multiamplitude CPM. The proposed algorithm can then be applied for reduction of PAPR. Similarly, QAM constellation can be expanded as proposed in [5] and the proposed algorithm can be used for reduction of PAPR.

Conclusions: The PAPR of OFDM-CPM signals can be reduced by >4 dB when multiamplitude CPM signals are used along with partial transmit sequences. The complexity and overhead of the proposed algorithm is minimal and no additional information need be transmitted. The proposed algorithm is also applicable to OFDM-PSK and -QAM signals for reduction of PAPR.

5 December 2001
Electronics Letters Online No: 20020613
DOI: 10.1049/el:20020613

I.A. Tasadduq and R.K. Rao (*Department of Electrical & Computer Engineering, Elborn College, 1201 Western Road, The University of Western Ontario, London, ON N6G 1H1, Canada*)

E-mail: iatasadd@uwo.ca

References

1 MÜLLER, S.H., and HUBER, J.B.: 'OFDM with reduced peak-to-average power ratio by optimum combination of partial transmit sequences', *Electron. Lett.*, 1997, **33**, (5), pp. 368–369
2 CIMINI, L.J., Jr. and SOLLENBERGER, N.R.: 'Peak-to-average power ratio reduction of an OFDM signal using partial transmit sequences', *IEEE Commun. Lett.*, 2000, **4**, (3), pp. 86–88
3 JONES, A.E., WILKINSON, T.A., and BARTON, S.K.: 'Block coding scheme for reduction of peak to mean envelope power ratio of multicarrier transmission schemes', *Electron. Lett.*, 1994, **30**, (25), pp. 2098–2099
4 OCHIAI, H., and IMAI, H.: 'MDPSK-OFDM with highly power-efficient block codes for frequency-selective fading channels', *IEEE Trans. Veh. Technol.*, 2000, **49**, (1), pp. 74–82
5 HWANG, C.-S.: 'Peak power reduction method for multicarrier transmission', *Electron. Lett.*, 2001, **37**, (17), pp. 1075–1077
6 PROAKIS, J.G.: 'Digital communications' (McGraw Hill Inc., 2001)

Traffic and physical layer effects on packet scheduling design in W-CDMA systems

J. Pérez-Romero, O. Sallent and R. Agustí

In the framework of 3G systems, the adoption of efficient packet scheduling algorithms is needed to guarantee QoS as well as to provide high capacity. Here, it is revealed that for a proper system optimisation, different packet scheduling strategies should be used depending on the deployment scenario (macrocell, microcell, picocell), the link direction (uplink or downlink), as well as the service characteristics (continuous, bursty traffic).

Introduction: W-CDMA packet based networks, such as those considered in the UTRA proposal [1], provide an inherent flexibility to handle the provision of future 3G mobile multimedia services. Radio resource management (RRM) entity is responsible for utilisation of the air interface resources and, consequently, the adoption of efficient RRM algorithms is needed to guarantee QoS as well as to provide high capacity. Packet scheduling is one of the RRM functions that will help to achieve such objectives.

In wireless environments, the problem of QoS provisioning for multimedia traffic has attracted interest in the literature in recent years [2, 3]. However, little effort has been devoted to date to addressing the RRM topic to guarantee a given QoS in a packet-driven environment such as the above-mentioned in the framework of the 3G systems. It is worth mentioning that RRM functions can be implemented in many different ways, this having an expected impact on the overall system efficiency and on the operator infrastructure cost, so that RRM strategies will definitely play an important role in a mature UMTS scenario. In addition, RRM strategies are not the subject of standardisation, and therefore these can be a differentiation issue among equipment producers and operators.

Packet scheduling strategies: The packet scheduling function shares the available air interface capacity between packet users. The packet scheduler can decide the allocated bit rates and the duration of the allocation. In W-CDMA this can be done in two ways [4, 5]: 'code scheduling', where a large number of users can have a low bit rate channel available simultaneously, and 'time scheduling', where capacity is given to a few number of users at each moment of time so that the user can have a very high bit rate but can use it only during small time periods.

It is generally accepted that the design of an efficient packet scheduler is a difficult task that typically involves a large number of conflicting requirements (maximisation of throughput, minimisation of packet losses, etc.) which must be analysed and weighted before a balanced and fair solution can be found. Our purpose in this Letter is to point out that, in addition to the above issues, in defining a packet scheduler it is necessary to consider a number of system aspects, e.g. the service characteristics (in terms of traffic generation patterns). In addition, the design of a layer 3 issue (radio resource) is influenced by a number of physical layer effects (layer 1). Consequently, a network operator seeking to optimise spectrum utilisation should implement different packet scheduling algorithms according to the specific scenario.

System model and results: Characteristics of the cellular model are taken from [6]. The Gaussian hypothesis and perfect power control are assumed for W-CDMA interference characterisation. Since the interest here is to focus on the scheduling process, traffic is supported through dedicated channels (DCH) [7].

To study the impact of the operation scenario, different orthogonality factor (ρ) values will be assumed [4] to represent different multipath propagation conditions (e.g. in microcells there is less multipath propagation and thus a better orthogonality). The orthogonality factor value also represents the link direction (for UTRA-FDD [1] $\rho = 1$ for the uplink since codes used by different users are not orthogonal, while $\rho \leq 1$ for the downlink since signals are orthogonally transmitted from the base station using OVSF codes). Note that the intracell interference is given by ρP, P being the received power from the own cell (e.g. $\rho = 0$ means that W-CDMA signals are perfectly orthogonals and they do not cause interference to each other).

The traffic model considered represents a typical interactive session, with several activity periods followed by thinking time periods. Within an activity period, several packet arrivals occur. To study the impact of the packet length on the packet scheduling strategies, the case of long packets is represented by an average length of 5000 bytes with a lognormal distribution, whereas the case of short packets is represented by an average 400 bytes [8].

Simulations are run for the case of long packets and short packets. In both cases several orthogonality factors are considered ($\rho = 1$, 0.6 and 0.3) and results are obtained for code scheduling as well as for time scheduling. In summarising the results obtained, Tables 1 and 2 focus only in terms of capacity (number of supported users under controlled performance) as a basis for comparisons.

Table 1: Capacity for 'code' and 'time' scheduling in case of long packets

Long packets	Capacity	Capacity	Capacity gain time against code scheduling (%)
	Time scheduling	Code scheduling	
$\rho = 1$	775	575	35
$\rho = 0.6$	1025	950	8
$\rho = 0.3$	1550	1525	1

For long packets, a time scheduling policy offers better performance than a code scheduling policy, denoting that it is not suitable to occupy